Ordered mesoporous molecular sieves synthesized by a liquid-crystal template mechanism

C. T. Kresge*, M. E. Leonowicz*, W. J. Roth*, J. C. Vartuli* & J. S. Beck†

Mobil Research and Development Corporation,
* Paulsboro Research Laboratory, Paulsboro, New Jersey 08066, USA
† Central Research Laboratory, Princeton, New Jersey 08543, USA

MICROPOROUS and mesoporous inorganic solids (with pore diameters of ≤20 Å and ~20–500 Å respectively)[1] have found great utility as catalysts and sorption media because of their large internal surface area. Typical microporous materials are the crystalline framework solids, such as zeolites[2], but the largest pore dimensions found so far are ~10–12 Å for some metallophosphates[3–5] and ~14 Å for the mineral cacoxenite[6]. Examples of mesoporous solids include silicas[7] and modified layered materials[8–11], but these are invariably amorphous or paracrystalline, with pores that are irregularly spaced and broadly distributed in size[8,12]. Pore size can be controlled by intercalation of layered silicates with a surfactant species[9,13], but the final product retains, in part, the layered nature of the precursor material. Here we report the synthesis of mesoporous solids from the calcination of aluminosilicate gels in the presence of surfactants. The material[14,15] possesses regular arrays of uniform channels, the dimensions of which can be tailored (in the range 16 Å to 100 Å or more) through the choice of surfactant, auxiliary chemicals and reaction conditions. We propose that the formation of these materials takes place by means of a liquid-crystal 'templating' mechanism, in which the silicate material forms inorganic walls between ordered surfactant micelles.

Members of this family of materials, designated MCM-41, were first observed in electron micrographs of products from hydrothermal reactions of aluminosilicate gels in the presence of quaternary ammonium surfactants. We prepared the MCM-41 molecular sieve characterized here as follows: 200 g of a solution containing 26 wt% hexadecyltrimethylammonium ion, as $C_{16}H_{33}(CH_3)_3N^+OH/Cl$ (~30% hydroxide), was combined with 2 g of Catapal alumina, 100 g of tetramethylammonium silicate solution (10% SiO_2, ratio of tetramethylammonium to $SiO_2 = 1$) and 25 g of a precipitated silica (HiSil), with stirring (molar ratio of $C_{16}H_{33}(CH_3)_3N^+$ to Si ≤ 1). This mixture was placed in a static autoclave at 150 °C for 48 hours. After cooling it to room temperature, we recovered the solid product by filtration on a Buchner funnel, washed it with water and dried it in air at ambient temperature. The as-synthesized product was then calcined at 540 °C for one hour in flowing nitrogen, followed by six hours in flowing air. The as-synthesized product contains over 40 wt% of the original surfactant as reflected by its composition (molar): 1 N, 19.6 C, 4.7 Si, 0.27 Al. In general, no special precautions (heating rate, atmosphere) are needed during the temperature ramping (from ambient temperature) and calcination processes.

Transmission electron microscopy (Fig. 1a) shows the regular hexagonal array of uniform channels characteristic of MCM-41. A representative electron diffraction pattern (Fig. 1*b*), with the MCM-41 in the same orientation, confirms the periodicity of the structure. For the sample described above, an interplanar spacing $d_{100} \approx 40$ Å was observed. In the corresponding powder X-ray diffraction pattern of the bulk sample (Fig. 2), the four peaks observed in the low-angle 2θ region can be indexed on a hexagonal unit cell with $a \approx 45$ Å ($2d_{100}/\sqrt{3}$). Generally, both electron and X-ray diffraction patterns show only a few low-order members of the *hk*0 subset of hexagonal reflections. The BET surface area of the preparation is ≥1,000 $m^2 g^{-1}$ with exceptionally high sorption capacities of >50 wt% cyclohexane at 40 torr, 49 wt% *n*-hexane at 40 torr, and 67 wt% benzene at 50 torr. The pore volume of this sample is 0.79 $cm^3 g^{-1}$. The range of pore volumes for MCM-41 samples is 0.7–1.2 $cm^3 g^{-1}$. Figure 3 shows N_2 adsorption isotherms for this material and for an amorphous mesoporous silica. The morphology of MCM-41 depends on synthesis conditions, but it is possible to obtain relatively large (~2 μm) hexagonal prisms of MCM-41, as seen in the scanning electron micrograph in Fig. 4.

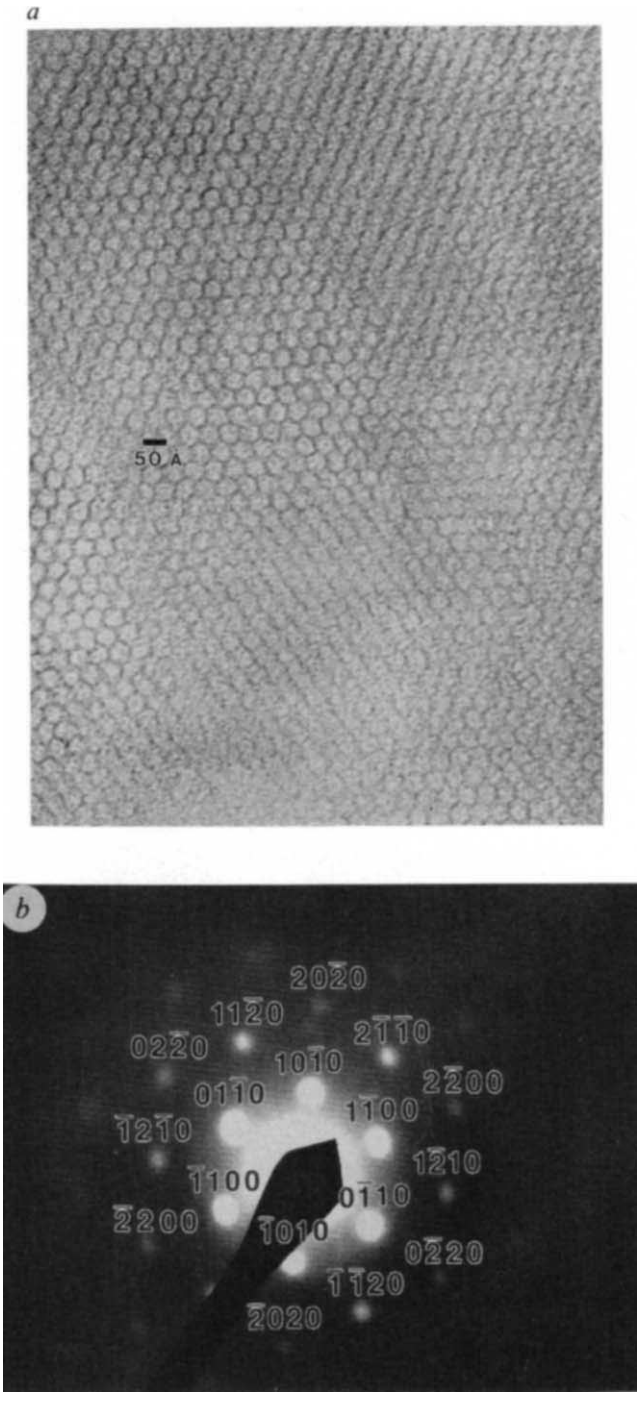

FIG. 1 *a*, Representative transmission electron micrograph of MCM-41. This image was obtained with a JEOL 200CX transmission electron microscope operated at 200 kV from a thin section prepared by ultramicrotomy. The instrument has an interpretable resolution of 4.5 Å and an effective 2-Å objective aperture was used to enhance image contrast. *b*, Representative electron micrograph of MCM-41. Selected area electron diffraction pattern indexed as the *hk*0 projection of a hexagonal unit cell with $a = 45$ Å.

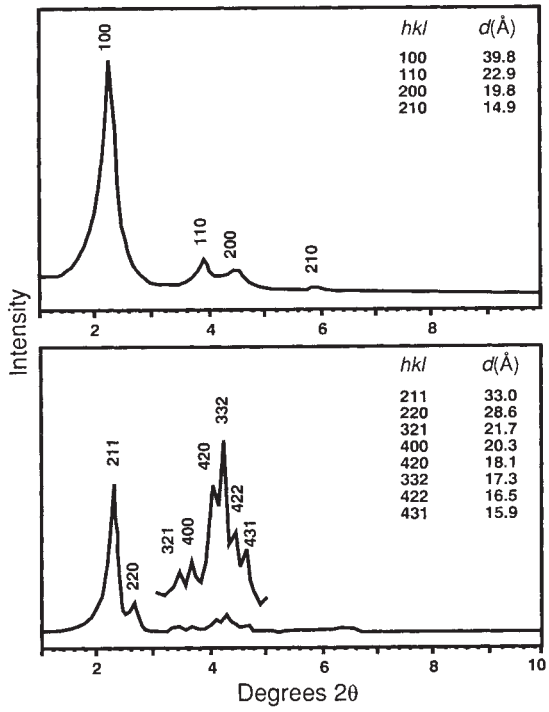

FIG. 2 *a*, Representative X-ray diffraction pattern of MCM-41. The pattern was obtained from a Scintag PAD automated diffraction system using Θ-Θ geometry, Cu Kα radiation ($\lambda = 1.5418$ Å) and an energy-dispersive detector. *b*, Representative X-ray diffraction pattern of cubic (*Ia*3*d*) phase. Inset is expansion of region $2\Theta = 3$–$5°$.

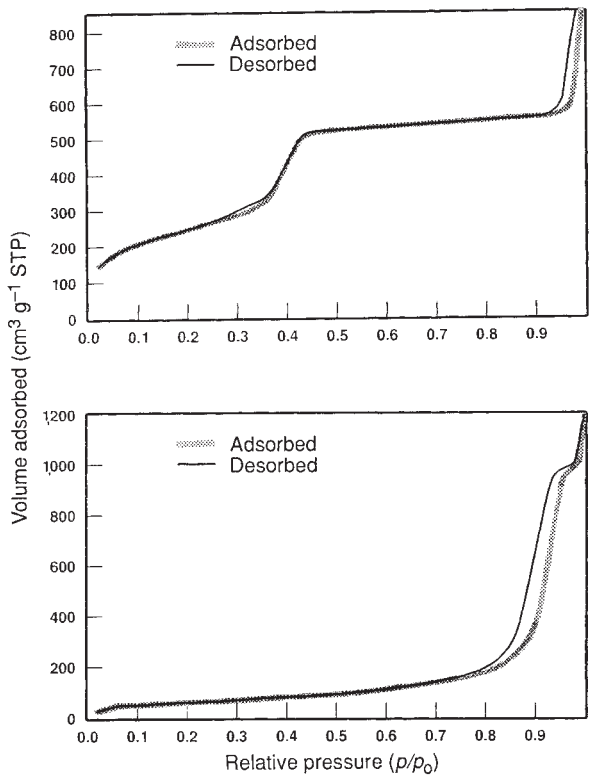

FIG. 3 *a*, N_2 adsorption isotherm for MCM-41. *b*, N_2 adsorption isotherm for amorphous silica (BET surface area 306 $m^2 g^{-1}$). These isotherms were obtained on a Micromeritics Digisorb 2600 adsorption instrument using standard procedures. The isotherm for this MCM-41 shows the inflection characteristic of capillary condensation within the pores, where the p/p_0 (relative N_2 pressure) position of the inflection point is related to the diameter of the pore being filled[26,27] ~40 Å. The significant adsorption at lower p/p_0 (~200 $cm^3 g^{-1}$) is most probably due to monolayer coverage of the walls and not to the presence of microporous phases.

The nature of the ordering in the walls of MCM-41—that is, the degree to which the atoms are precisely ordered—is not fully understood. We have not detected any X-ray diffraction peaks with a non-zero *l* component. The large, regular pore channels of these materials would, however, make the *hk*0 reflections dominate, resulting in little scattering intensity along the *c*-axis.

The pore diameter of MCM-41 can be varied by changing the alkyl chain length of the cationic surfactants used in the synthesis procedure. For example, by substituting the dodecyltrimethylammonium ion ($C_{12}H_{25}(CH_3)_3N^+$) for hexadecyltrimethylammonium ion, we produced a sample of MCM-41 with 30-Å pore diameter. The C/N molar ratio for as-synthesized C_{12}-based MCM-41 is 15, which is consistent with the surfactant remaining intact. Another way of altering the pore diameter of MCM-41 is to add auxiliary hydrocarbons, such as alkylated benzene (for example 1,3,5-trimethylbenzene), to the synthesis mixture[16]. The incremental addition of 1,3,5-trimethylbenzene results in the concomitant increase of d_{100} and the pore diameter. Hexagonal phases with pore diameters up to ~100 Å have been characterized.

The microscopy and diffraction results presented above are

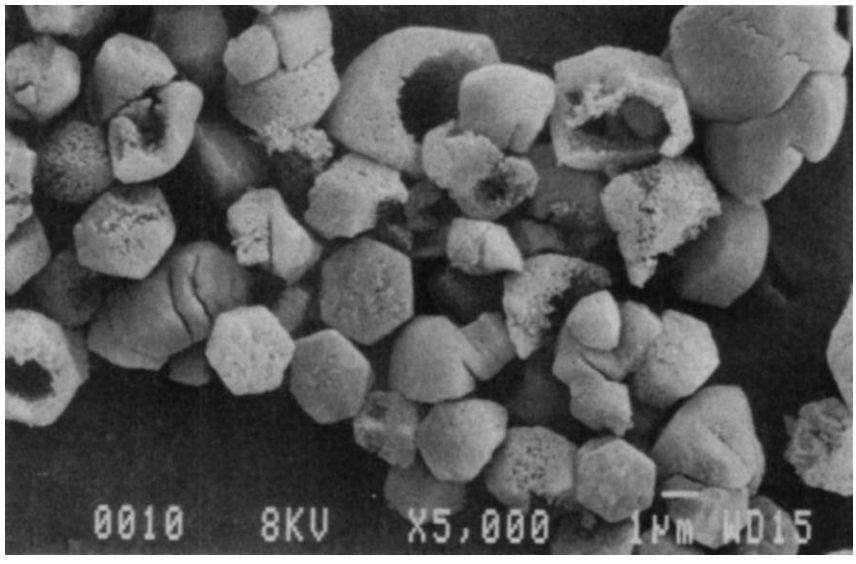

FIG. 4 Scanning electron micrograph of a MCM-41 sample. This micrograph was obtained on a JEOL JXA-840 scanning electron microscope using conventional sample preparation and imaging techniques.

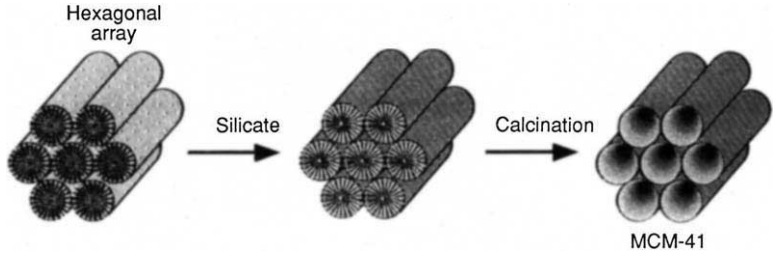

FIG. 5 Schematic drawing of the liquid-crystal templating mechanism. Hexagonal arrays of cylindrical micelles form (possibly mediated by the presence of silicate ions), with the polar groups of the surfactants (light grey) to the outside. Silicate species (dark grey) then occupy the spaces between the cylinders. The final calcination step burns off the original organic material, leaving hollow cylinders of inorganic material.

strikingly similar (R. M. Dessau and C. D. Chang, personal communication) to those obtained[17-19] from lyotropic liquid-crystal phases which are produced in surfactant–water mixtures. These phases are ordered arrays of surfactant aggregates which occur at specific amphiphile concentrations[20,21]. One such phase, the 'middle' or 'H_I' phase, produces transmission electron microscope images[22] analogous to those of MCM-41. The H_I phase is a hexagonal array of cylindrical micelles in which the hydrophobic hydrocarbon chains are gathered in the centre and the polar groups are arrayed on the surface, in contact with a continuous region of water surrounding the micelles[20]. The repeat dimensions of the MCM-41 prepared as described above are consistent with those determined for hexadecyltrimethylammonium-based liquid crystals, where cylinder-to-cylinder repeat distances of ~40 Å have been observed[20].

The observed dependence on alkyl chain length and the influence of auxiliary organic molecules on the resultant inorganic product are also consistent with two phenomena observed for liquid crystals. The diameter of hexagonal liquid-crystal phases prepared with anionic surfactants depends on the alkyl chain length of the surfactant[20,21]. Organic species may be solubilized inside the hydrophobic regions of micelles, causing an increase in micelle diameter[21,23]. Chemicals added to surfactant solutions can increase the porosity of amorphous adsorbants[24].

These similarities suggest that these mesoporous molecular sieves are formed by a 'liquid-crystal templating' mechanism. In this mechanism (Fig. 5), inorganic material occupies the continuous solvent (water) region to create inorganic walls between the surfactant cylinders. It may be that encapsulation occurs because anionic aluminosilicate species enter the solvent region to balance the cationic hydrophilic surfaces of the micelles. Alternatively, it may be the introduction of the aluminosilicate species themselves that mediates the hexagonal ordering. Once an ordered array is established, subsequent thermal processing is used to remove the organic material and produce a stable mesoporous molecular sieve.

Although other workers[13] have produced mesoporous silicates with high surface areas, the mechanism used has been the intercalation of a guest (such as hexadecyltrimethylammonium chloride) into a layered host (such as kanemite). The mesopores of these materials are not an ordered regular array (as observed in MCM-41). The final product retains, in part, the layered nature of the kanemite precursor. Furthermore, the concentrations, reagents, pH and reaction conditions are not conducive for liquid-crystal formation and templating.

Additional strong evidence for the proposed liquid-crystal templating mechanism is the discovery of another member of this family[14,15] that mimics a liquid-crystal structure[25]. A representative powder X-ray diffraction pattern of a silicate molecular sieve with cubic symmetry ($Ia3d$) is given in Fig. 2. The cubic phase is prepared by increasing the molar ratio of $C_{16}H_{33}(CH_3)_3N^+$ to Si to values greater than one. □

Received 1 May; accepted 1 September 1992.

1. IUPAC Manual of Symbols and Terminology *Pure appl. Chem.* **31,** 578 (1972).
2. Meier, W. M. & Olson, D. H. *Atlas of Zeolite Structure Types,* 2nd Edn (Butterworths, London, 1988).
3. Davis, M. E., Saldarriaga, C., Montes, C., Garces, J. & Crowder, C. *Nature* **331,** 698–699 (1988).
4. Dessau, R. M., Schlenker, J. L. & Higgins, J. B. *Zeolites* **10,** 522–524 (1990).
5. Estermann, M., McCusker, L. B., Baerlocher, C., Merrouche, A. & Kessler, H. *Nature* **352,** 320–323 (1991).
6. Moore, P. B. & Shen, J. *Nature* **306,** 356–358 (1983).
7. Iler, R. K. *The Chemistry of Silica* (Wiley, New York, 1979).
8. Pinnavaia, T. J. *Science* **220,** 365–371 (1983).
9. Landis, M. E. *et al. J. Am. chem. Soc.* **113,** 3189–3190, 1991.
10. Vaughan, D. E. W. & Lussier, R. J. *Proc. 5th int. Conf. Zeolites* (ed. Rees, L. V. C.) 94–100 (Heyden, London, 1980).
11. Vaughan, D. E. W. *Am. chem. Soc. Symp. Series* **368,** 308–325 (1988).
12. Tindwa, R. M., Ellis, D. K., Peng, G. Z. & Clearfield, A. *J. chem. Soc. Faraday Trans. 1,* **81,** 545–548 (1985).
13. Yanagisawa, T., Shimizu, T., Kazuyuki, K. & Kato, C. *Bull. Chem. Soc. Jpn* **63,** 988–992 (1990).
14. Kresge, C. T., Leonowicz, M. E., Roth, W. J. & Vartuli, J. C. *U.S. Patent No. 5,098,684* (1992); *U.S. Patent No. 5,102,643* (1992).
15. Beck, J. S. *et al. U.S. Patent No. 5,108,725* (1992).
16. Beck, J. S. *U.S. Patent No. 5,057, 296* (1991).
17. Ekwall, P. *Advances in Liquid Crystals,* Vol. 1 (ed. Brown, G. H.) (Academic, New York, 1971).
18. Ekwall, P., Mandell, L. & Fontell, K. *Liquid Crystals* (ed. Brown, G. H.) 325–334 (Gordon and Breach, London, 1969).
19. Luzzati, V. *Biological Membranes* (ed. Chapman, D.) 71–123 (Academic, New York, 1968).
20. Tiddy, G. J. T. *Phys. Rep.* **57,** No. 1, 1–46 (1980).
21. Winsor, P. A. *Chem. Rev.* **68,** No. 1, 1–40 (1968).
22. Goodman, J. F. & Clunie, J. S. *Electron Microscopy of Liquid Crystals, Liquid Crystals and Plastic Crystals,* Vol. 2 (eds. Gray, G. W. & Winsor, P. A.) 1–23 (Wiley, New York, 1974).
23. Speght, P. P. A., Skoulios, A. E. & Luzzati, V. *Acta cryst.* **14,** 866–872 (1961).
24. Komarov, V. S. & Kuznetsova, T. F. *Vesti Akad. Navuk BSSR* No. 2, 22–27 (1978).
25. Luzzati, V. & Speght, P. P. A. *Nature* **215,** 701–704, 1967.
26. Gregg, S. J. & Sing, K. S. W. *Adsorption, Surface Area, and Porosity,* 2nd Edn (Academic, New York, 1982).
27. Barrett, E. P., Joyner, L. G. & Halenda, P. P. *J. Am. chem. Soc.* **73,** 373–380 (1951).

ACKNOWLEDGEMENTS. We thank the technical staff of the Paulsboro and Central Research Laboratories, Mobil Research and Development Corporation, for discussions. In particular, we thank C. D. Chang, R. M. Dessau and H. M. Princen for alerting us to references and for discussions, D. T. Geston and K. G. Simmons for assistance, J. B. Higgins and N. H. Goeke for the scanning electron micrograph, J. L. Schienker for assistance in X-ray diffraction pattern indexing and Mobil Research and Development Corporation for its support.

Anthropogenic influence on the distribution of tropospheric sulphate aerosol

J. Langner*, H. Rodhe†, P. J. Crutzen‡ & P. Zimmermann‡

* Swedish Meteorological and Hydrological Institute, S-601 76 Norrköping, Sweden
† Department of Meteorology, Stockholm University, S-106 91 Stockholm, Sweden
‡ Max-Planck Institute for Chemistry, P.O. Box 3060, D-6500 Mainz, Germany

HUMAN activities have increased global emissions of sulphur gases by about a factor of three during the past century, leading to increased sulphate aerosol concentrations, mainly in the Northern Hemisphere. Sulphate aerosols can affect the climate directly, by increasing the backscattering of solar radiation in cloud-free air, and indirectly, by providing additional cloud condensation nuclei[1–4]. Here we use a global transport–chemistry model to estimate the changes in the distribution of tropospheric sulphate aerosol and deposition of non-seasalt sulphur that have occurred since pre-industrial times. The increase in sulphate aerosol concentration is small over the Southern Hemisphere oceans, but reaches a factor of 100 over northern Europe in winter. Our calculations indicate, however, that at most 6% of the anthropogenic sulphur emissions is available for the formation of